

Inlet Liner Design for aircraft air conditioning system

Frank Simon¹, Fabien Méry, Rémi Roncen, Lucas Pascal, Delphine Sebbane, Estelle Piot
ONERA/DMPE - Université de Toulouse
F-31055, Toulouse, France

ABSTRACT

With regard to the reduction of aircraft noise, so-called acoustic liners are generally based on a (micro-) perforated plate above a honeycomb. They are developed to absorb waves propagated along, for example, engine nacelles or air conditioning systems. Their design must take into account the dimensional and phenomenological characteristics of constituent materials, manufacturing and assembly specifications and industrial requirements involving multiphysical phenomena. Indeed, they are submitted to high sound pressure level, shear turbulent grazing flow and potentially high temperatures. That is the reason why there is a need to design liners thanks to an optimization loop combining numerical and experimental tools. This paper describes an ONERA optimization process (OPAL platform) coupling: firstly, a 1D/2D Linear Euler Equation models evaluates acoustic Transmission Loss along a lined duct in shear and hot flow; secondly, a 1D propagation code determines an impedance surface above porous multilayered structures; thirdly, an evolutionary computation algorithm optimizes the liner impedance; fourthly, an experimental database may provide initial flow characteristics and assess the target impedance. This process is applied to a liner with a perforated plate extended by hollow tubes (LEONAR concept) to absorb low frequency noise generated by a jet pump of an air conditioning system.

Keywords: Liner, Optimisation, impedance

I-INCE Classification of Subject Number: 37

1. INTRODUCTION

Acoustic treatments used along engine nacelles or air conditioning systems are characterized by the reduction of acoustic power associated with their specific area. They are also subject to operational requirements in terms of aerodynamic impact, mass, thickness, temperature, static and vibration behavior, fire resistance, drainage... (cf. EUROCAE [1]). In practice, the liner design implies an optimization process with acoustic objective functions, such as impedance or transmission loss (TL), while taking into account the dimensional and phenomenological characteristics of materials (porous layer, resonator...), manufacturing, assembly specifications and industrial constraints.

¹ frank.simon@onera.fr

However, most of designs led by laboratories are based on classical architecture with reference models applied under restrictive conditions. It appears necessary to implement numerical and experimentation tools with an iterative or even an optimization process in order to propose configurations able to satisfy required constraints.

This paper describes a process set up in ONERA, in the form of a tool platform (acronym OPAL), which allows (Figure 1):

- to simulate the acoustic TL along a lined duct in shear and hot flow with an impedance surface provided by porous multilayered structures
- to determine the optimal impedance relative to TL under various constraints with an evolutionary computation algorithm
- to assess the target impedance or adjust characteristics of materials with aeroacoustic specific tests.

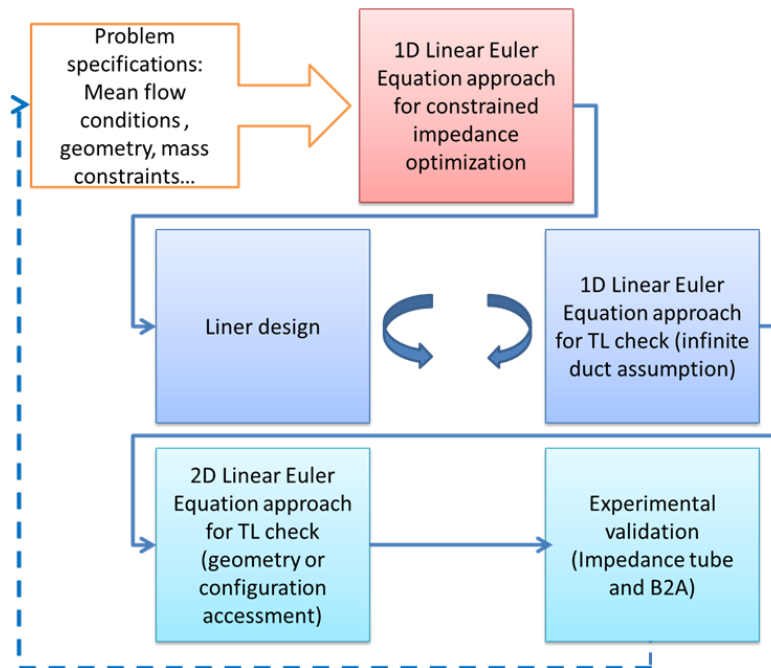


Figure 1: Chart of OPAL platform

An example of application is provided to mitigate the noise source generated by an aircraft air conditioning system. Until now, acoustic liners for fan-based systems are made of porous materials, very efficient for sound absorption in the high-frequency range while addressing the weight and space requirements. For the air pump system, the liner design is much more challenging because of the lower range of frequency to be dealt with, which is conflicting with the low thickness requirement. A breakthrough in the liner concept design and manufacturing is therefore necessary. The proposed solution for low frequency range uses the principle of LEONAR concept [2].

2. OPAL PLATFORM

2.1 1D/2D Linear Euler Equation models for acoustic Transmission Loss

Let us consider an inviscid perfect gas flowing along an infinitely long cylindrical duct of radius R . Let t be the time, x , r and θ the axial, radial and azimuthal coordinates respectively, U_x , U_r and U_θ the axial, radial and azimuthal components of the velocity vector U , p the pressure, ρ the density and s the entropy per unit mass. $\gamma = C_p/C_v$ represents the ratio of specific heat capacities at constant pressure and

constant volume respectively. The pressure, the density and the absolute temperature T satisfy the equation of state $p = \rho r T$, with $r = C_p - C_v$. Then, if D/Dt stands for the convective derivation $\partial/\partial t + (U \cdot \nabla)$, the Euler equations read

$$\frac{\partial \rho}{\partial t} + \nabla \cdot (\rho U) = 0, \quad \rho \frac{DU}{Dt} + \nabla p = 0, \quad \frac{Ds}{Dt} = 0 \quad (1)$$

The flow field is written as the sum of a steady base flow and a small-amplitude unsteady perturbation:

$$(U, p, \rho) = (U, p_0/\gamma, \rho_0) + (u', p', \rho') \quad (2)$$

The base flow is assumed streamwise-invariant and axisymmetric, which means that:

$$U_x = U_x(r), \quad U_r = 0, \quad U_\theta = 0, \quad \rho_0 = \rho_0(r) \quad (3)$$

In order to obtain the linearized Euler equations, small amplitude disturbance fields is sought for under harmonic formation

$$(u'_x, u'_r, u'_\theta, p', \rho') = (U'_x, U'_r, U'_\theta, P', \Xi') \exp(i(\omega t - kx - m\theta)) \quad (4)$$

where $\omega = 2\pi f$ is the pulsation frequency, k the complex wave number and m the azimuthal wave number. The velocity, pressure and density disturbance $(U'_x, U'_r, U'_\theta, P', \Xi')$ are unknown functions of r . The entropy equation simplifies the system and assumes that $P = \Xi$, the linearised Euler equations for mass and momentum can be written as follows:

$$L(k, \omega) \cdot X = 0 \quad (5)$$

where L is a linear operator and $X = (P', U'_x, U'_r, U'_\theta)$. m is fixed and ω and k must be fit to consider either a spatial or a temporal eigenvalue problem (usually, for acoustics issues, a spatial eigenvalue problem is considered, i.e. ω is a given real frequency).

Concerning the boundary conditions, the duct wall can be constituted of either a locally reacting liner of complex specific impedance Z or a rigid wall ($Z \rightarrow \infty$ or $U'_r = 0$ at the wall). Solving this linear problem with the boundary condition for a fixed azimuthal wavenumber m , a known mean velocity and density profile and impedance Z implies solving a dispersion relation:

$$D(k, \omega, m) = 0 \quad (6)$$

This generalized eigenvalue problem $M.X = \mu Q.X$ can be solved thanks to the MAMOUT code [3], in which the equations are discretized along the radial direction through a spectral collocation method (Tchebychech polynomials) or through a compact finite-difference scheme (Gamet scheme, of order 6 on a regular mesh). The resolution of such an eigenvalue problem enables to compute cut-on modes but also cut-off modes, in both directions of propagation (downstream and upstream).

The description of the pressure field (Figure 2) inside a cylindrical duct is written as a series expansion of Fourier-Bessel:

$$p(x, r, \theta) = \sum_{m=-\infty}^{\infty} \sum_{n=1}^{\infty} [A_{m,n} e^{-ik_{m,n}^+ x} + B_{m,n} e^{+ik_{m,n}^- x}] \varphi_{m,n}(r) e^{im\theta} \quad (7)$$

where $A_{m,n}$ and $B_{m,n}$ are respectively the complex amplitudes of an incident and reflected mode (m,n) (if incident wave propagates in the direction of flow).

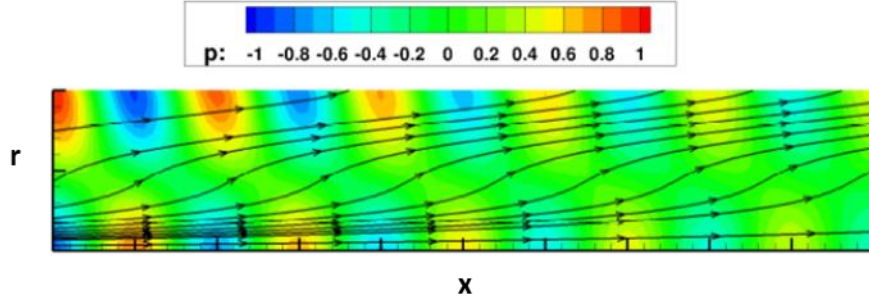


Figure 2: Propagation of an acoustic mode in an infinite lined duct in flow and energy streamlines

Regarding a given cut-on left running mode (m,n) , and considering an impedance value, the transmission loss coefficient (dB/m) can be directly derived from the imaginary part of $k_{m,n}$ (Figure 3):

$$TL_{m,n}/m = 20 \log_{10} \left(\frac{p(x=1)}{p(x=0)} \right) = -20 \log_{10}(e) \text{Im}(k_{m,n}) \approx -8.6859 \text{Im}(k_{m,n}) \quad (8)$$

In order to present the results applied to a considered problem, this value is multiplied by the real duct length to obtain a realistic value of transmission loss through the lined duct.

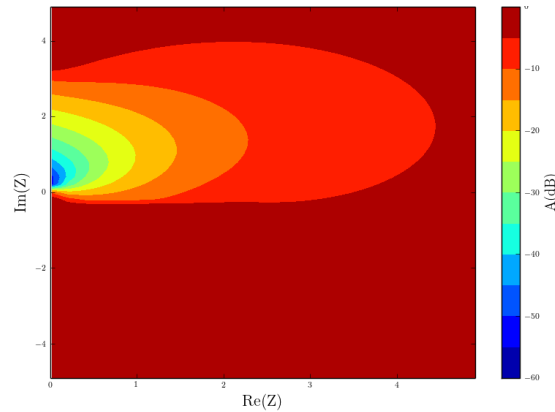


Figure 3: Ex. of Transmission loss mapping for a given mode (m,n) and frequency.

Nevertheless, the resulting lining discontinuities cannot be accounted for by one-dimensional analysis. Similarly, the one-dimensional approach is not intended to be used for cases where the acoustic treatment in the cross-section of a duct is not azimuthally uniform.

For these two kinds of lining non-uniformities (either axially or azimuthally), it is necessary to account for an additional dimension when solving the linearised Euler Equations. The solver EMILE [4,5], based on ELVIN [6,7], solves the linearised Euler equations on a two-dimensional mesh by means of the discontinuous Galerkin method.

2.2 1D propagation code to determine an impedance surface above porous multilayered structures

Most materials used in aeroacoustic applications for noise reduction are multilayered. A conventional liner is, for instance, made of a perforated plate backed by an air cavity (Figure 4).

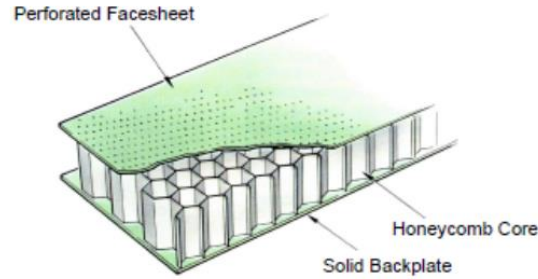


Figure 4: Sketch of conventional liner

To represent the acoustic behavior of such materials, the use of a transfer matrix approach is generally adopted. One represents every component of the material as a 2x2 matrix relating the acoustic pressure and normal velocity at each interface of the material. Thus, in OPAL platform, each layer is represented as an “equivalent fluid”, thus allowing a simple representation.

Semi-phenomenological modeling of porous media

In the simplified case where a porous material is assumed rigid, only airborne waves propagate in the material. The contribution of the solid phase to the acoustics is negligible and one can see the porous medium as an equivalent fluid subject to visco-inertial and thermal losses due to the high surface contact ratio between the fluid and solid phases and to the complex shape of the pores. Following [12] and assuming total decoupling between visco-inertial and thermal effects, one obtains the complex-valued Helmholtz equation of linear acoustics controlling the time harmonic wave propagation inside the equivalent-fluid material:

$$\Delta p + \omega^2 \frac{\bar{\rho}_{eq}}{\bar{K}_{eq}} p = 0 \quad (9)$$

where $\bar{\rho}_{eq}$ is the equivalent complex density of the fluid, encompassing all the viscous effects between the two phases, and \bar{K}_{eq} is the equivalent complex bulk modulus of the fluid, encompassing all the thermal effects inside the pores. Semi-phenomenological models for $\bar{\rho}_{eq}$ and \bar{K}_{eq} are obtained for different simplified pore geometries by using the limits of low or high frequency regimes, where the fluid is fully viscous-isothermal or potential-adiabatic, respectively. Thus, the JCAPL model [13,14,15,16] takes into account cross-section variations and possible moderate constrictions between the pores.

The equivalent fluid modeling has been extended to perforated plates and screens in [17]. Correction lengths due to acoustic radiation and viscous reactance in the vicinity of the perforations depend on the type of medium in contact. These interfacing effects were included in an equivalent tortuosity of the perforated plate. The parameters of the JCAPL are not all useful here, due to the geometrical simplicity of perforated plates and screens compared to more complex porous media. It can be replaced by JCA model [13,14].

“By-design” modeling of long tube resonators

The case of resonators LEONAR with hollow long tubes can be designed by another approach [2]. Indeed, the propagation of waves along hollow tubes can be represented as a linear combination of propagational, thermal and viscous modes [8]. The pressure in the propagational mode satisfies an ordinary wave equation, while the temperature and velocity in the other modes satisfy diffusion equations.

The pressure field p along each narrow channel is mainly due to the propagational mode, for harmonic time dependence (expressed by ω), with solutions in the form:

$$p(x, r) = A \cos(\bar{k}_r r) (e^{i\bar{k}x} + e^{-i\bar{k}x}) \quad (10)$$

with r and x , respectively the radial and axial coordinates, \bar{k}_r and \bar{k} , respectively the complex radial and axial wavenumbers.

k_r , parameter common to all modes, can be inferred from the mathematical expression of transverse velocities due to propagational, thermal and viscous modes. Indeed, as the sum of transverse velocities must vanish at the inner boundaries, the transverse propagation constant (with the assumption of narrow channels: $\bar{k}_r r_i \ll 1$ or $\cos(\bar{k}_r r_i) \approx 1$) is given by:

$$\bar{k}_r^2 = -\left(\frac{\omega}{c}\right)^2 \frac{(\gamma - 1)F(k_h r_i) + F(k_v r_i)}{1 - F(k_v r_i)} \quad \text{where} \quad F(X) = \frac{\tan(X)}{X} \quad (11)$$

with k_h and k_v , respectively thermal and viscous boundary layer thicknesses.

The complex propagation constant in the axial direction of the channel \bar{k} and the characteristic impedance \bar{Z}_c are determined simply by:

$$\bar{k} = \left(\frac{\omega}{c}\right) \sqrt{\frac{1 + (\gamma - 1)F(k_h r_i)}{1 - F(k_v r_i)}}, \quad \bar{Z}_c = \frac{\rho \omega}{\bar{k} (1 - f_v)} \quad (12)$$

For circular tubes, one must introduce $r_i/2$ in $F(X)$, instead of r_i [2]. Classical inductive and resistive end corrections can also be added for a specific impedance [9], but the effects are relatively negligible for long tubes and low frequencies.

Transfer matrix approach

Connecting two layers can be done simply by knowing the acoustic pressure and velocity at each interface and by using a transfer matrix \mathbf{T} [8]:

$$\begin{bmatrix} p_{x=0} \\ u_{x=0} \end{bmatrix} = \mathbf{T}_{(\omega)} \begin{bmatrix} p_{x=d} \\ u_{x=d} \end{bmatrix} \quad (13)$$

where d is the material thickness, p is the pressure and u the velocity normal to the interface.

- In the case of an homogeneous” equivalent fluid layer” with a semi-phenomenological modeling of porous media, one has:

$$T(\omega) = \begin{bmatrix} \cos(\bar{k}_{eq} d) & i \bar{Z}_{eq} \sin(\bar{k}_{eq} d) \\ i \sin(\bar{k}_{eq} d) / \bar{Z}_{eq} & \cos(\bar{k}_{eq} d) \end{bmatrix} \quad (14)$$

In the previous equation, $\bar{Z}_{eq} = \bar{\rho}_{eq} \bar{c}_{eq}$ with $\bar{c}_{eq} = \sqrt{\bar{K}_{eq} / \bar{\rho}_{eq}}$ the equivalent speed of sound inside the layer, and $\bar{k}_{eq} = \omega / \bar{c}_{eq}$ the equivalent wave number.

- In the case of an homogeneous” equivalent fluid layer” for long tube resonators, one has:

$$T(\omega) = \begin{bmatrix} \cos(\bar{k} d) & i \bar{Z}_c \sin(\bar{k} d) \\ i \sin(\bar{k} d) / \bar{Z}_c & \cos(\bar{k} d) \end{bmatrix} \quad (15)$$

To obtain the transfer matrix of a multi-layer material, one simply multiplies the elementary matrices together, as

$$T(\omega) = T_1(\omega) I_{12}(\omega) T_2(\omega) \quad (16)$$

where $T(\omega)$ is the obtained total matrix, $T_1(\omega)$ is the matrix associated to the first layer, $T_2(\omega)$ the matrix of the second layer, and $I_{12}(\omega)$ a coupling matrix taking into account materials of different porosities.

Then, the normal surface impedance of the multi-layer material, having a total transfer matrix T , is simply obtained, where ϕ the porosity of the upper layer, as:

$$Z_s(\omega) = -\frac{T_{22}(\omega)}{\phi T_{21}(\omega)} \quad (17)$$

2.3 Optimisation approach

For each frequency, a cost function is a sum of the Transmission Loss of cut-on modes for different azimuthal and radial modes. In order to minimize this cost function, an evolutionary computation algorithm can be used to have a flexible algorithm that can be widely fitted with some other constrains. Indeed, the goal of these numerical simulations is to find the best impedance with an absorption coefficient over a given value in order to ensure the efficiency of the liner. For that, a death penalty method is applied, i.e. each candidate under a threshold fixed value of normal absorption is rejected. This method of eliminating infeasible solutions from a population may work reasonably well when the feasible search space is convex and it constitutes a reasonable part of the whole search space.

3. Experimental Setups

Validation are carried out in an impedance tube (without flow) and in a grazing flow aeracoustic test bench (B2A).

B2A is made of a stainless steel tube of section 50 mm x 50 mm whose the termination is equipped with a quasi-anechoic outlet (Figure 5). A mean flow of bulk Mach number up to 0.3 can be provided. In the test section, this flow shows fully developed turbulent boundary layers. Two acoustic drivers mounted upstream of the test section are used to

generate tones (usually multi-sine signal) at up to 140 dB over a frequency range of 0.3 to 3.5 kHz (i.e., the no-flow cut-off frequency of the duct). Sixteen microphone locations are available in the upper wall (opposite the liner) to measure the acoustic pressure field from upstream of the liner leading edge to downstream of the liner trailing edge. Flush-mounted B&K 4182 microphone probes are used. Usually, only two upstream locations are considered to measure the amplitude of the incident acoustic plane waves. However, for the pressure-based impedance eduction method, one microphone probe is moved along the whole set of microphone locations. A two-component fringe mode Laser Doppler Velocimetry allows the measurement of the axial and transverse velocity components (mean, turbulent, acoustic) in almost the entire volume of the test section. The emitting optics produce a 50 μm -diameter measurement volume. Flow is seeded with either incense smoke or amorphous silica particles. The LDV database is used as input of a velocity-based impedance eduction method.

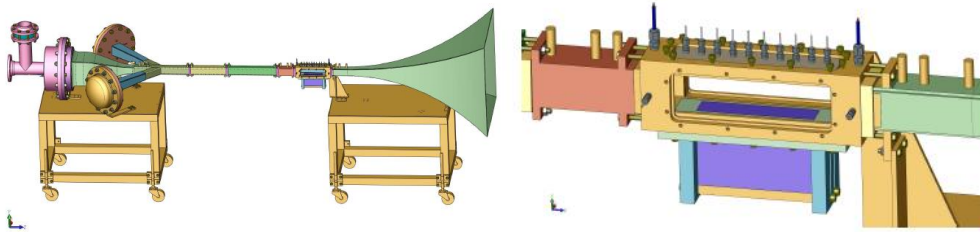


Figure 5: The Aero-thermo-acoustic bench B2A.

Obtaining the numerical acoustic fields necessary for the impedance eduction strategy requires solving the equations of acoustic propagation in the presence of a grazing flow. To do so, the two-dimensional time-harmonic LEE are solved thanks to a discontinuous Galerkin (DG) scheme [10].

The inverse problem is defined by the minimization of the following objective function:

$$\mathcal{J}_{red} = \frac{\int_{\Omega_{obs}} \{\varphi|_{DG} - \varphi|_{Meas}\}^T \{\bar{\varphi}|_{DG} - \bar{\varphi}|_{Meas}\} dx dz}{\int_{\Omega_{obs}} \|\varphi|_{Meas}\|^2 dx dz} \quad (18)$$

where Ω_{obs} is the observation region.

When the impedance eduction method is based on acoustic pressure measurements on the wall opposite the test liner, Ω_{obs} is made of the discrete set of microphone locations at the wall, and only the pressure component of the state vector is considered in the objective function.

When the impedance eduction method is based on LDV measurements above the test liner (Figure 6), Ω_{obs} is a rectangular ($x; z$) region and the ($u; v$) velocity components of the state vector are considered in previous function.

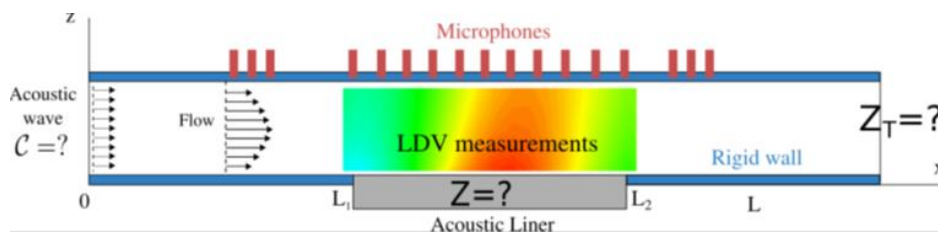


Figure 6: Impedance eduction from LDV or pressure measurements.

A determinist approach, based on BFGS-B (Broyden, Fletcher, Goldfarb, Shanno for bounded variables) algorithm [10], or a statistical approach, based on Bayes' theorem are used to solve the optimization problem [11].

Finally, static pressure measurements are performed in the upper wall, with a SVMtec pressure multisensor, to determine the pressure drop in the B2A test section then an apparent friction velocity [18] relative to the liner. Indeed, the friction velocity is a driving parameter regarding the effect of the flow on the acoustic resistance of the liner. The liner surface has to be as smooth as possible in order to reduce the acoustic resistance increase due to the grazing flow.

4. Example of OPAL platform application

The methodology is applied to a jet pump composed of an inlet, a mixing part and a diffuser part which is the part to line (Figure 7).

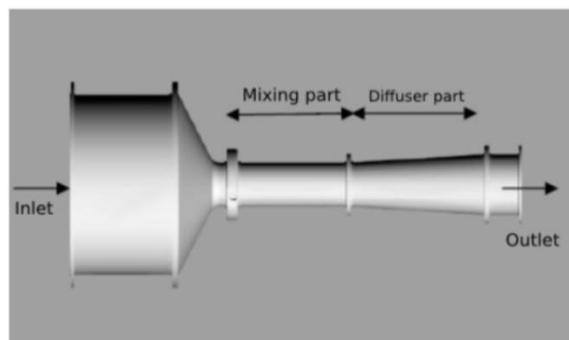


Figure 7: Sketch of the Jet Pump.

The interesting frequencies for this problem range from 200 Hz up to 5000Hz. The measured spectra out of this jet pump exhibit high sound pressure levels in all this frequency range. The noise induced by this jet pump is more likely to be broadband noise with no preferred frequency. The liners design process that has been performed during the IDEAS project takes into account the real shear flow for several typical flow configurations.

To validate the relevance of OPAL platform, a Low Frequency liner (LF) based on LEONAR concept is assumed from a perforated surface coupled with tubes of variable lengths inserted in separated back cavities. Two tube lengths are chosen to provide an acoustic attenuation between 500 and 800 Hz for a limited thickness h (Figure 8).

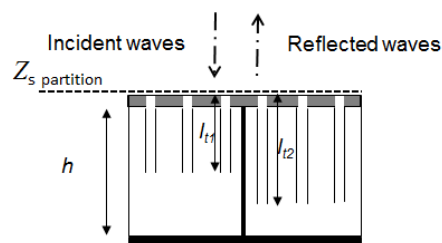


Figure 8: Physical configurations of LEONAR with an upper perforated plate connected to two types of hollow tubes (lengths l_{t1} and l_{t2}) inserted in cavities with identical thickness h .

After an iterative process based on a maximal TL (without flow) with a threshold fixed value of normal absorption, impedance tube and B2A samples have been manufactured

in resin by Polyshape through an additive manufacturing process (Figure 9). The nature of resin has been chosen to satisfy temperature constraints.

The measurement of absorption coefficient in impedance tube shows a low dependence on the incident SPL (between 115 and 135 dB) (Figure 10). Simulation with “By-design” modelling appears relatively predictive with frequency discrepancies lower than 5%.

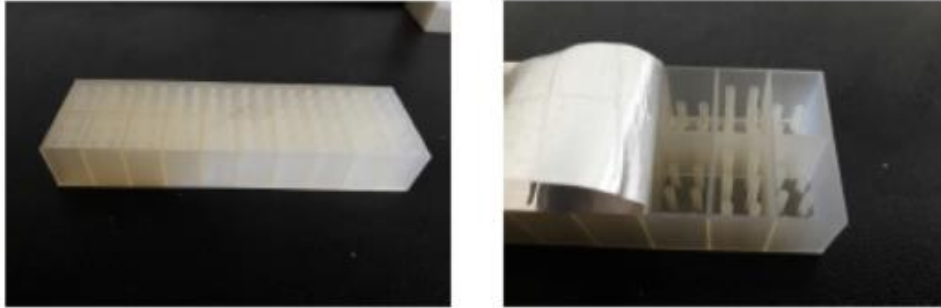


Figure 9: View of liner sample for B2A (top and bottom)

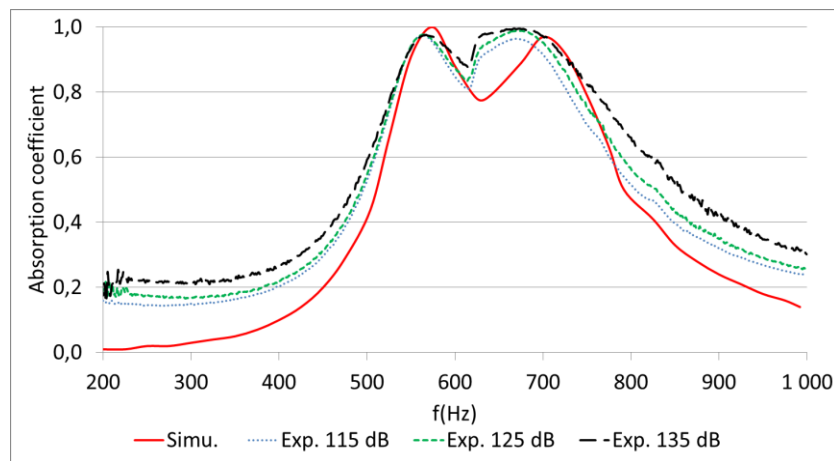


Figure 10: Theoretical and experimental absorption coefficient of LF liner for different incident SPL.

Impedance reduction tests led by LDV for several Mach numbers bring to light a flow effect on the induced resistance (Figure 11). As mentioned before, the measured fiction velocity value is a relevant parameter to assess this influence (in this case, respectively 2.39 and 3.18 m/s for $M=0.15$ and 0.2). A way to reduce this one and, so on, the induced resistance is to increase the liner porosity [19]. Besides, when added to linear models, the non-linear resistance based on porosity appears representative to real behavior in flow (Figure 12). Corresponding TL/m (dB) obtained theoretically with a Poiseuille Boundary layer (Figure 13) shows a significant decrease of attenuation if the cost function does not take into account the mean flow. Therefore, another optimization process is necessary to provide a high TL in presence of flow, while respecting industrial constraints. However, at this stage, the methodology appears satisfying to converge to a Low-frequency liner applied to a jet pump.

CONCLUSIONS

A tool platform (called OPAL) has been implemented at ONERA in order to optimize aeronautic acoustic liners under various industrial constraints. To this end, 1D/2D Linear Euler models solving a modal duct Transmission Loss have been coupled with impedance models based on equivalent fluid layers and a Transfer Matrix

approach. The optimization process follows an evolutionary computation algorithm. Moreover, aeroacoustic experiments are part of this loop, not only to assess the target impedance but also to provide input (boundary layer, friction velocity...). The methodology is applied to a jet pump with specifications as high Transmission Loss with shear flow, in low frequency range, with a small thickness and temperature constraints. In the future, other constraints (or cost functions) as mass, manufacturing discrepancies, minimal hygrometry rate should enrich the process.

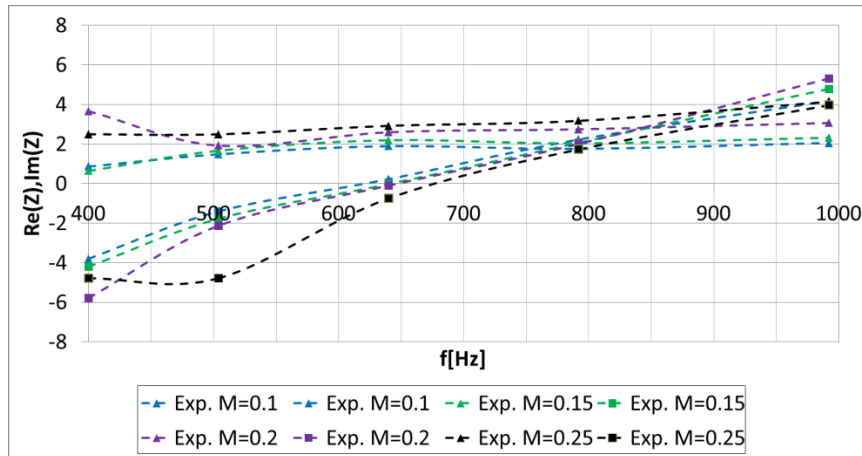


Figure 11: Experimental impedance of LF liner for different Mach numbers.

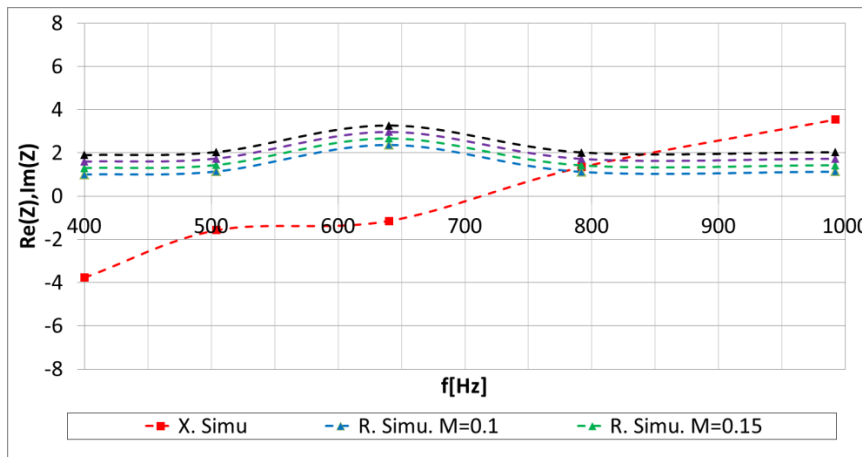


Figure 12: Theoretical impedance of LF liner for different Mach numbers.

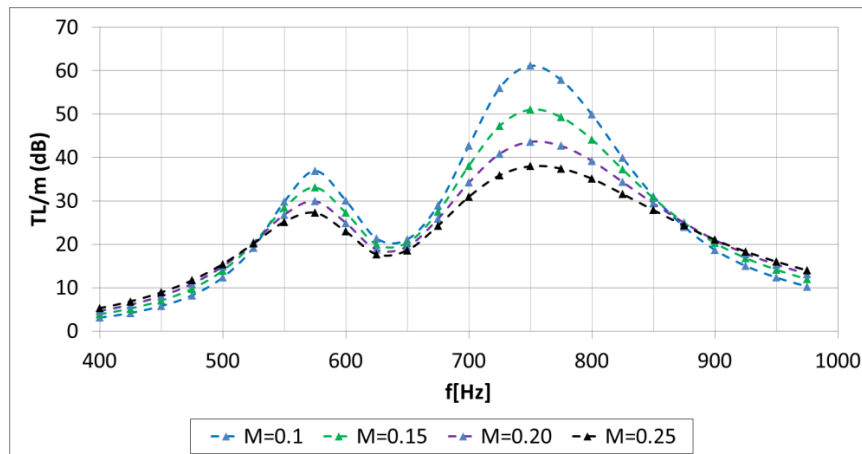


Figure 13: Theoretical TL/m (dB) of LF liner for different Mach numbers.

5. ACKNOWLEDGEMENTS

The research leading to these results has received funding from the Clean Sky Joint Undertaking through the IDEAS project (GA-716499).

6. REFERENCES

1. RTCA DO-160G, “*Environmental Conditions and test Procedures for Airborne Equipment*”.
2. F. Simon, “*Long Elastic Open Neck Acoustic Resonator for low frequency absorption*”, *J. Sound Vib.*, 421, 1-16, (2018).
3. G. Boyer, J.-P. Brazier, E. Piot, “*Theoretical investigation of hydrodynamic surface mode in a lined duct with sheared flow and comparison with experiment*”, *J. Sound Vib.*, 330, 1793–1809, (2011).
4. L. Pascal, E. Piot, G. Casalis, “*Discontinuous Galerkin method for acoustic modes computation in lined ducts*”, 18th AIAA/CEAS Aeroacoustics Conference, (2012)
5. L. Pascal, “*Acoustique modale et stabilité linéaire par une méthode numérique avancée. Cas d'un conduit traité acoustiquement en présence d'un écoulement*”, Ph.D. thesis, ISAE, (2013).
6. J. Primus, “*Détermination de l'impédance acoustique de matériaux absorbants en écoulement par méthode inverse et mesures LDV*”, Ph.D. thesis, INSA Toulouse, (2012).
7. J. Primus, E. Piot, F. Simon, “*An adjoint-based method for liner impedance education: validation and numerical investigation*”, *J. Sound Vib.*, 332, 58–75, (2013).
8. U. Ingard, “*Notes on "Sound absorption technology"*”, Version 94-02, ISBN 0-931784-28-X, (1994).
9. T. H. Melling, “*The acoustic impedance of perforates at medium and high sound pressure level*”, *J. Sound Vib.* 29(1), 1-65, (1973).
10. J. Primus, E. Piot, F. Simon, “*An adjoint-based method for liner impedance education: Validation and numerical investigation*”, *J. Sound Vib.*, 332(1), (2013).
11. R. Roncen, F. Méry, E. Piot, F. Simon, “*Statistical Inference of Liner Impedance with Shear Grazing Flow*”, 24th AIAA/CEAS Aeroacoustics Conference, (2018).
12. C. Zwikker, C. W. Kosten, “*Sound absorbing materials*”, Elsevier, New York, (1949).
13. D. L. Johnson, J. Koplik, R. Dashen, “*Theory of dynamic permeability and tortuosity in fluid-saturated porous media*”, *J. Fluid Mech.*, 176, 379–402, (1987).
14. Y. Champoux, J.-F. Allard, “*Dynamic tortuosity and bulk modulus in air-saturated porous media*”, *J. Appl. Acoust.*, 70 (4), 1975–1979, (1991).
15. S. R. Pride, F. D. Morgan, A. F. Gangi, “*Drag forces of porous-medium acoustics*”, *Phys. Rev. B*, 47 (9), 4964–4978, (1993).
16. D. Lafarge, “*Propagation du son dans les matériaux poreux à structure rigide saturés par un fluide viscothermique: Définition de paramètres géométriques, analogie électromagnétique, temps de relaxation*”, Ph.D. thesis, Université du Maine, (1993).
17. N. Atalla, F. Sgard, “*Modeling of perforated plates and screens using rigid frame porous models*”, *J. Sound Vib.*, 303 (1-2), 195–208, (2007).
18. H. Schlichting, “*Boundary layer theory*”, McGraw-Hill classic textbook reissue, 1979.
19. A. B. Bauer, “*Impedance theory and measurements on porous acoustic liners*”, *J. Aircr.* 14, 720–728, (1977).